Online Measurement of Magnetron Rieke Reflection Coefficient

Vladimir Bilik

Faculty of Electrical Engineering and Information Technology, Slovak University of Technology
Ilkovicova 3, 81219 Bratislava, Slovak Republic
E-mail: vladimir.bilik@s-team.sk

Introduction

The frequency f_g generated by a magnetron and net power P_L delivered to its load depend on the load reflection coefficient as perceived by the magnetron. By convention, this quantity, henceforth termed the *Rieke reflection coefficient*, is defined as the reflection coefficient $\Gamma_R = |\Gamma_R| \exp(j\varphi_R)$ observed looking toward the load in a specific rectangular waveguide arrangement called the *reference launcher* (Fig. 1), the dimensions of which are provided in magnetron datasheets. The reference launcher specified by essentially all manufacturers of 2.45-GHz magnetrons with powers up to about 2 kW uses a waveguide with unusual inner dimensions $a_r = 95.3$ mm (not shown in Fig. 1), $b_r = 54.6$ mm. The reference plane for Γ_R measurement is the plane R of the magnetron antenna axis.
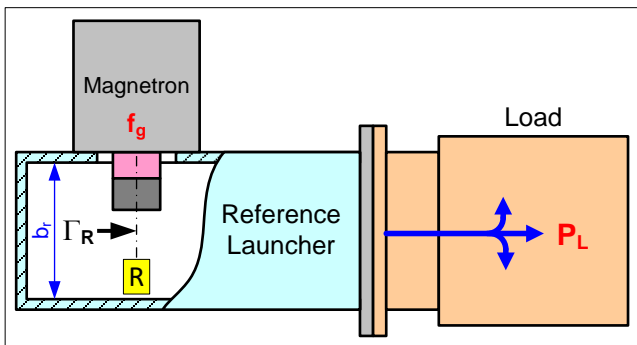
Figure 1: Magnetron in a reference launcher. A definition of the Rieke reflection coefficient Γ_R.

The dependence of f_g and P_L on Γ_R is visualized in the form of a *Rieke diagram*[1], which is a rotated polar chart in the complex plane of Γ_R displaying a family of contours of constant f_g and of constant P_L (Fig. 2). An applicator design goal is to restrict Γ_R to be within the range where the magnetron behaves properly (the area covered by the contours).

Using a reference launcher in a real installation may be inconvenient due to its uncommon waveguide dimensions. Practical installations employ standard waveguide types and prefer customized launchers based on the same waveguides. Aside from the reference arrangement, Γ_R may not be directly observable. However, we still need to refer to Γ_R to predict the magnetron behavior in *arbitrary* arrangements. This does not pose a principal problem in low-power experiments, such as in experiment-assisted applicator design, because in this case, an *antenna probe* can be utilized, enabling standard vector network analyzers to measure Γ_R even on a swept basis[2].
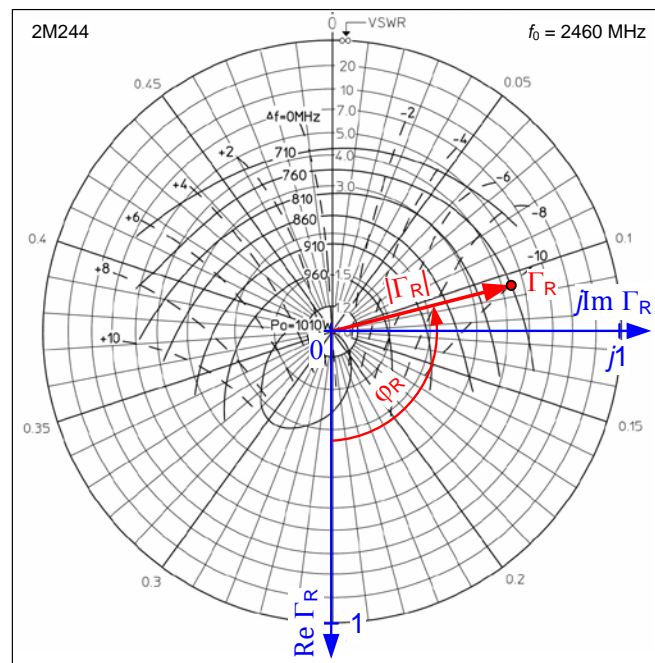
Figure 2: Rieke diagram of 2M244 magnetron. For the indicated $\Gamma_R = 0.638 \angle 104.4°$, the generated frequency f_g is 2,450 MHz (note the 2,460 MHz reference frequency), and the delivered power P_L is 760 W.

Difficulties arise when we seek to measure Γ_R online (Fig. 3), i.e. in the course of real operation of an installation powered by the magnetron. There exist high-power vector reflectometers (HPVR) based on standard waveguide types, that are capable of measuring the applicator reflection coefficient Γ_A at a certain plane A under full magnetron power. However, because the arrangement in Fig. 3 differs from the reference arrangement of Fig. 1, the measured Γ_A differs from the Rieke reflection coefficient Γ_R. One possible way to resolve this problem is to establish a relation between Γ_A and Γ_R, enabling Γ_R to be computed from a measured Γ_A. In this paper, we develop a procedure to arrive at such a relation and present some experimental results for its verification.
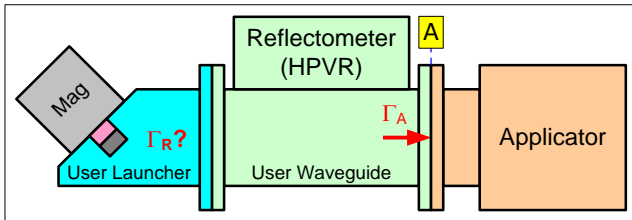
Figure 3. Installation with a customized launcher and a high-power vector reflectometer (HPVR).

Theory

The method for finding a relation between the magnetron Rieke reflection coefficient Γ_R and an arbitrarily measured load reflection coefficient Γ_A in a user arrangement is based on a comparison of the two scenarios depicted in Fig. 4.

Case (a) shows the reference arrangement where a magnetron antenna probe associated with a given magnetron type is used in conjunction with the reference launcher. The probe input reflection coefficient Γ_p at a reference plane B is measured by a vector network analyzer (VNA). The load reflection coefficient Γ_R at plane R is, by definition, the Rieke reflection coefficient. The scattering matrix of the two-port circuit between planes B and R is S_R (Fig. 4c). The circuit is assumed to be linear and reciprocal.

Case (b) shows the same antenna probe installed in a customized user launcher in an arrangement that also incorporates a high-power vector reflectometer (HPVR). The load (applicator) reflection coefficient Γ_A, defined at plane A, is regarded as known because in full-power operation it will be measured directly by HPVR. The scattering matrix of the circuit between planes B and A is S_A (Fig. 4d).
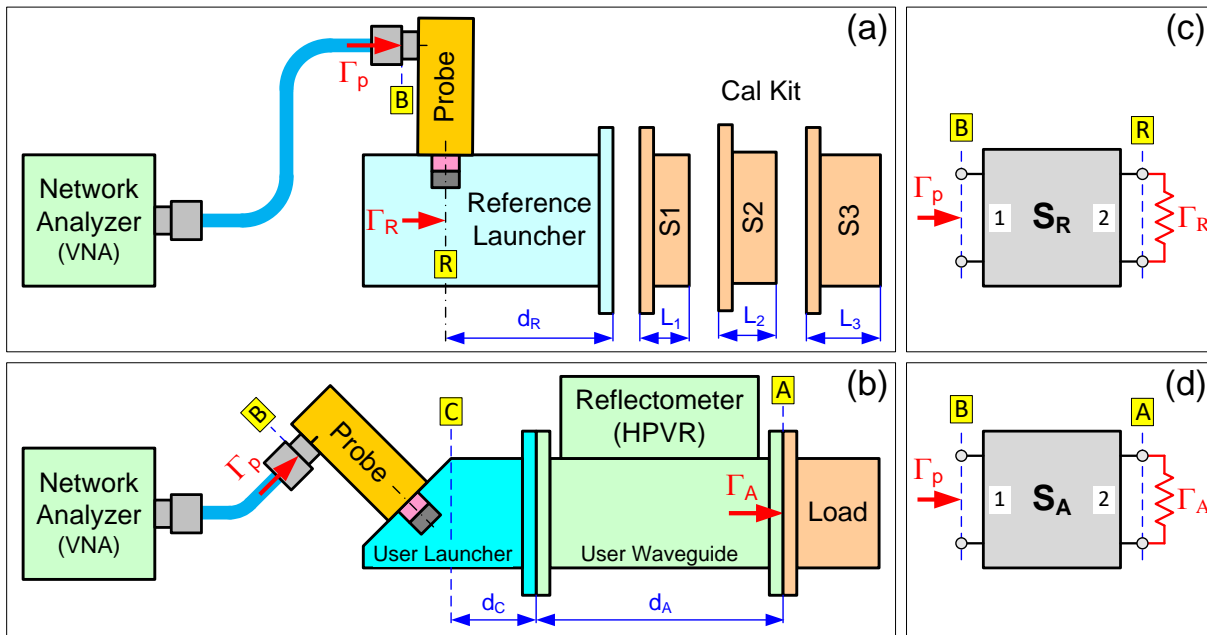
Figure 4. Measurement setups using a magnetron probe in the reference and user arrangements.

For case (a), the relation between Γ_p and Γ_R is given by[3]

$$\Gamma_p = \frac{-D_R\Gamma_R + S_{R11}}{-S_{R22}\Gamma_R + 1} , \qquad (1)$$

where S_{Rij} are the elements of matrix $\mathbf{S_R}$, and $D_R = S_{R11}S_{R22} - S_{R12}S_{R21}$ is its determinant. Due to circuit reciprocity, $S_{12} = S_{21}$. The setup (b) is topologically very similar to (a). Therefore, a relation similar to (1) must exist between Γ_p and Γ_A, only with the set of parameters S_{A11}, S_{A22}, D_A. Consequently,

$$\Gamma_p = \frac{-D_A\Gamma_A + S_{A11}}{-S_{A22}\Gamma_A + 1}, \qquad (2)$$

where $D_A = S_{A11}S_{A22} - S_{A12}S_{A21}$ is the determinant of scattering matrix $\mathbf{S_A}$.

Suppose that in both cases (a) and (b), the same reflection coefficient Γ_p is measured. Consequently, the magnetron in place of the antenna probe would also perceive the same load in both arrangements. Eliminating Γ_p by relating the right-hand sides of (1) and (2) will therefore yield the wanted link between Γ_A and Γ_R:

$$\frac{-D_R\Gamma_R + S_{R11}}{-S_{R22}\Gamma_R + 1} = \frac{-D_A\Gamma_A + S_{A11}}{-S_{A22}\Gamma_A + 1}. \qquad (3)$$

Solving for Γ_R, we obtain

$$\Gamma_R = \frac{a\Gamma_A + b}{c\Gamma_A + 1}, \qquad (4)$$

where

$$a = \frac{S_{R11}S_{A22} - D_A}{S_{A11}S_{R22} - D_R},$$

$$b = \frac{S_{A11} - S_{R11}}{S_{A11}S_{R22} - D_R}, \qquad (5a, b, c)$$

$$c = \frac{D_R S_{A22} - D_A S_{R22}}{S_{A11}S_{R22} - D_R}.$$

Note that all the quantities are complex and frequency-dependent. Equation (4) represents the sought relation, linking the full-power, online measurable applicator reflection coefficient Γ_A with the magnetron Rieke reflection coefficient Γ_R.

Determining the Scattering Parameters

The parameters S_{R11}, S_{R22}, D_R can be obtained by standard VNA one-port calibration methods[4], using, for instance, three offset reference launcher waveguide shorts for calibration standards, as indicated in Fig. 4a. More details about the optimal lengths of these shorts are available in our previous paper[2]. At plane R, the short reflection coefficients are

$$\Gamma_{Si}(f) = \exp j\left[\pi - \frac{4\pi(L_i + d_R)}{\lambda_{gr}(f)} \right] \qquad i = 1, 2, 3$$

where f is frequency, L_i are physical lengths of the shorts, d_R is the distance of plane R from the launcher output plane, and λ_{gr} is the reference launcher guide wavelength. The calibration consists of connecting in turn the three shorts, measuring for each short the probe input reflection coefficient Γ_{pi} ($i = 1, 2, 3$) in a frequency range of interest, and inserting Γ_{pi} into (1) along with the known $\Gamma_R = \Gamma_{Si}$ of the shorts. After simple manipulation, we thus obtain for each frequency a set of three complex linear equations

$$S_{R11} + S_{R22}\Gamma_{Si}\Gamma_{pi} - D_R\Gamma_{Si} = \Gamma_{pi} \qquad i = 1, 2, 3$$

The equations can be readily solved for the unknowns S_{R11}, S_{R22}, and D_R. More than three standards can be in principle used, yielding an overdetermined equation set, which can contribute to the accuracy of determining the unknowns.

The parameters S_{A11}, S_{A22}, D_A of the working installation according to Fig. 4b can be obtained by exactly the same procedure, except that the calibration standards must be based on the user waveguide. Normally, the standards are connected at the output flange of the user launcher while the calibration plane (C in Fig. 4b) may be located at a distance d_C inside it. Let the parameters thus obtained be S_{C11}, S_{C22}, D_C. If the Γ_A definition plane is spaced by distance d_A from the launcher output plane, then

$$S_{A11} = S_{C11} , \qquad S_{A22} = S_{C22}\exp(-2j\theta) ,$$

$$D_A = D_C\exp(-2j\theta), \qquad (6)$$

where $\theta = 4\pi(d_C + d_A)/\lambda_g$ is the (frequency-dependent) electrical distance between calibration

plane C and measurement plane A, and λ_g is the user guide wavelength.

Equivalent Two-Port

As an alternative to (4), the $\Gamma_A \rightarrow \Gamma_R$ transform can be expressed in terms of scattering parameters S_{ij} of a fictitious equivalent two-port circuit connected between reference planes R (port 1) and A (port 2). Then,

$$\Gamma_R = S_{11} + \frac{S_{12}S_{21}\Gamma_A}{1 - S_{22}\Gamma_A} = \frac{-D\Gamma_A + S_{11}}{-S_{22}\Gamma_A + 1}, \quad (7)$$

where $D = S_{11}S_{22} - S_{12}S_{21}$ is the determinant. Comparing (4) and (7), the equivalent S-parameters are

$$S_{11} = b \quad , \quad S_{22} = -c$$
$$S_{12} = S_{21} = \sqrt{a - bc} \exp(-jn\pi), \quad (8)$$

where a, b, c are given by (5) and n is an undetermined integer. Because the transform involves only the product $S_{12}S_{21}$, we can safely assume $n = 0$.

The usefulness of expressing the $\Gamma_A \rightarrow \Gamma_R$ conversion in terms of the S-parameters of an equivalent two-port lies in the fact that some HPVRs are capable of loading a file of such S-parameters, performing the mapping (7) internally,

and outputting immediately the Rieke reflection coefficient Γ_R. This enables real-time display of the magnetron load in the Rieke diagram during full-power operation of any equipment into which such HPVR can be installed.

Experiments

To verify the developed approach, two experimental setups (Fig. 5) were assembled, using a 2M244 magnetron. The setups extend those in Fig. 4 with the ability to realize any desired Γ_A by means of a 3-stub tuner. A WR340-based S-Team autotuner STHT 1.5 terminated in a waterload and controlled from a PC was used for this purpose. A well-matched ($|S_{11}| < -30$ dB) linear taper section with net taper length 86.5 mm has been inserted between the reference launcher and the autotuner.

In high-power experiments, the autotuner measures reflection coefficient Γ_A referred to plane A of stub S1, which is $d_h = 132.3$ mm apart from the autotuner input plane. In addition to Γ_A, the autotuner is capable of measuring frequency f_g generated by the magnetron and net power P_L absorbed in the load. These data are sufficient for determining or verifying a magnetron's Rieke diagram.
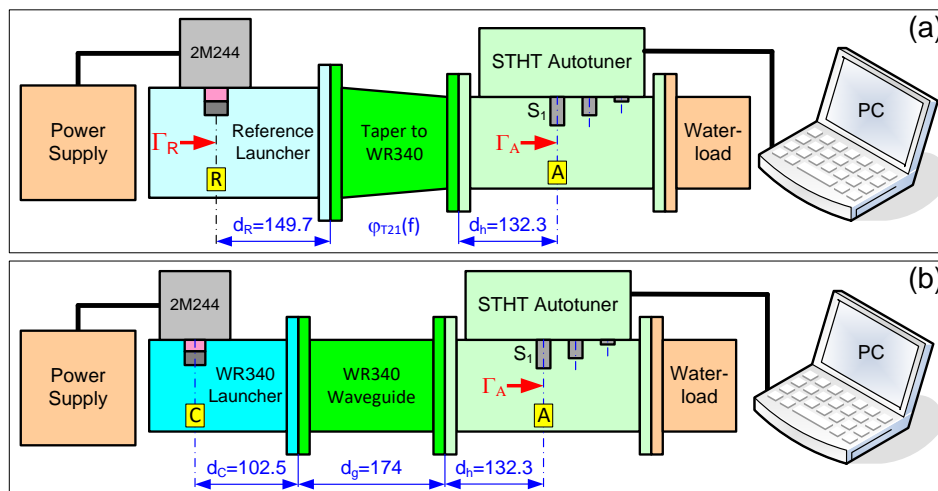
Figure 5. Two experimental arrangements.

To establish the scattering parameters of the equivalent transforming circuit, the launchers were detached from the waveguides and the magnetron was in turn replaced by a 2M244 antenna probe. A calibration was performed on either setup using a set of corresponding waveguide shorts. Reference plane B (Fig. 4) was defined by the coaxial short accessory to the antenna probe. Both calibrations

were performed in the range 2200 – 2700 MHz with step 1 MHz (501 points). The reference calibration setup (Fig. 4a) was exactly the same as described before[2], including the calibration shorts. The calibration yielded scattering matrix S_R, expressed in the form of a tabulated frequency dependence of parameters S_{R11}, S_{R22}, D_R.

The test arrangement (Fig. 5b) involved a WR340-based magnetron launcher made by IBF Electronic, a 174-mm long section of standard WR340 waveguide, the autotuner and a waterload. The calibration used an overdetermined set of four WR340 shorts with physical lengths

$$L_i = (i-1) \times 20.5 \text{ mm}, \; i = 1\ldots4,$$

connected in turn to the launcher output flange and electrically extended by 102.5 mm to the antenna axis plane C. The calibration yielded the frequency dependence of S_{C11}, S_{C22}, D_C. The parameters S_{A11}, S_{A22}, D_A were then obtained using (6) with $d_C = 102.5$ mm and $d_A = d_g + d_h = 306.3$ mm.

Following the two calibrations, the S-parameters of the $\Gamma_A \to \Gamma_R$ transformation circuit were computed using (5) and (8). Their frequency dependence is plotted in Fig. 6 (note that $S_{12} = S_{21}$ and that only the product $S_{12}S_{21}$ is employed in the transform equations).
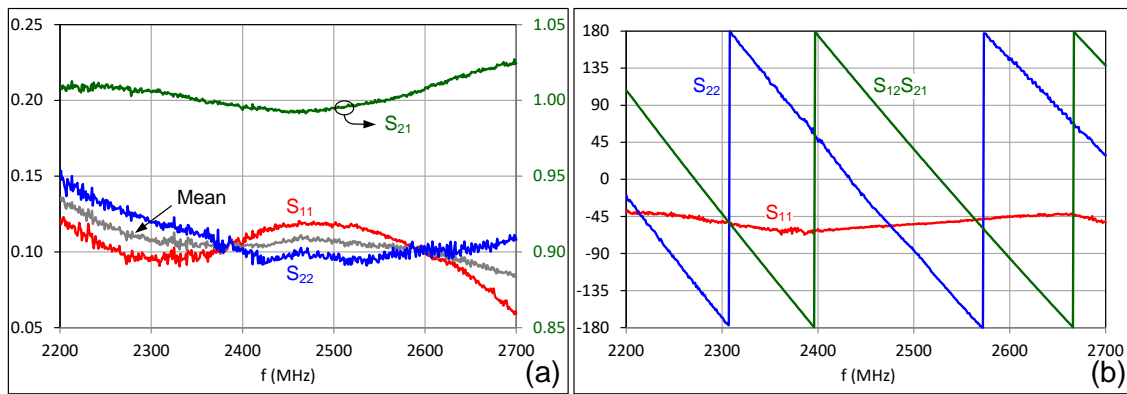
Figure 6. *S*-parameter magnitudes (a) and phases in degrees (b) of the transformation circuit. Phase of $S_{12}S_{21}$ product is plotted in (b).

The accuracy of the determined Γ_R can be probably enhanced by using the mean value $(|S_{11}| + |S_{22}|)/2$ instead of both $|S_{11}|$ and $|S_{22}|$ (the gray line in Fig. 6a) and setting $|S_{21}|$ to the theoretical unity. We have nevertheless used the original data because the deviations from the ideal are only on the order of ±0.01 in the ISM sub-band. In high-power experiments, the same 2M244 magnetron was used in turn in both setups. The magnetron was powered by a one-phase half-wave rectified high voltage power supply as stipulated in the 2M244 datasheet for the Rieke diagram definition.

For the measurement, the autotuner was set to the manual stubs control mode, and an assortment of as much as 150 loads with $|\Gamma_A| \le 0.75$ was synthesized by suitable tuning stubs insertions. At 2,460 MHz, the values of Γ_A would have created a regular rectangular grid. However, since the magnetron frequency is load-dependent, the

actually measured Γ_A would deviate, most markedly in the Rieke diagram's sink area.

To arrive at Γ_R using the test setup according to Fig. 5b, the obtained file of the S-parameters visualized in Fig. 6 was loaded to the PC control program, which then automatically performed the needed $\Gamma_A \to \Gamma_R$ conversion (7).

For comparison purposes, the reference setup in Fig. 5a was used for direct measurement of Γ_R because with the well matched taper, the $\Gamma_A \to \Gamma_R$ transform is merely a rotation (phase shift) of Γ_A by an angle proportional to the electric distance between planes R and A. Such a shift can also be represented by a transforming S-matrix, this time with parameters of the real circuit between planes R and A, i.e.

$$S_{11} = 0, \quad S_{22} = 0, \quad S_{12} = S_{21} = \exp(j\varphi_{21}),$$

$$\varphi_{21} = -2\pi d_R / \lambda_{gr} + \varphi_{T21} - 2\pi d_h / \lambda_g,$$

where the distances d_R, d_h are defined in Fig. 5a, λ_{gr} is the launcher guide wavelength, λ_g is the WR340 guide wavelength, and φ_{T21} is the phase of the taper transmission coefficient S_{21}. The phase φ_{T21} was determined by both measurement and electromagnetic simulation; the difference was less than 1° in 2,400 – 2,500 MHz range.

Results in condensed form are presented in Fig. 7, which shows (in a normally oriented polar chart) the Rieke reflection coefficients obtained for both the reference arrangement of Fig. 5a (yellow circles) and the test arrangement of Fig. 5b (black squares). Also drawn (green solid lines) are the contours of constant f_g and of constant P_L copied from the 2M244 datasheet.
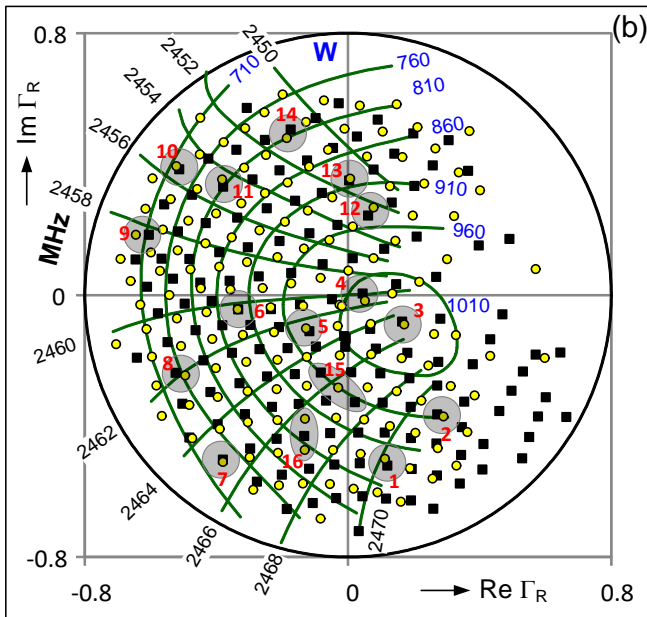
Figure 7. Rieke reflection coefficients obtained by direct method (circles) and by the proposed method (squares). Numbered points in shaded circles and ellipses were used for comparison.

While the collection of tuning stub insertions is the same in both setups, different sets of Γ_R are generated because the transforming circuits differ. For comparison purposes, we chose 14 cases for which Γ_R obtained from both setups well coincide. In Fig. 7, these points are numbered 1 to 14 and surrounded by shaded circles. Added are two cases (15 and 16) enabling a simple interpolation. The same Γ_R should in both setups cause the magnetron

to generate the same frequency f_g and deliver the same power P_L. Their differences, shown as solid lines in Fig. 8, can therefore serve as a validity check of the proposed method. Figure 8a reveals that the frequency difference is within ±2 MHz. The RMS deviation is less than 1 MHz, which is about 5% of the magnetron frequency span. Figure 8b shows that the power difference is within ±100 W. The RMS deviation is about 30 W, which is 3% of the magnetron nominal power.
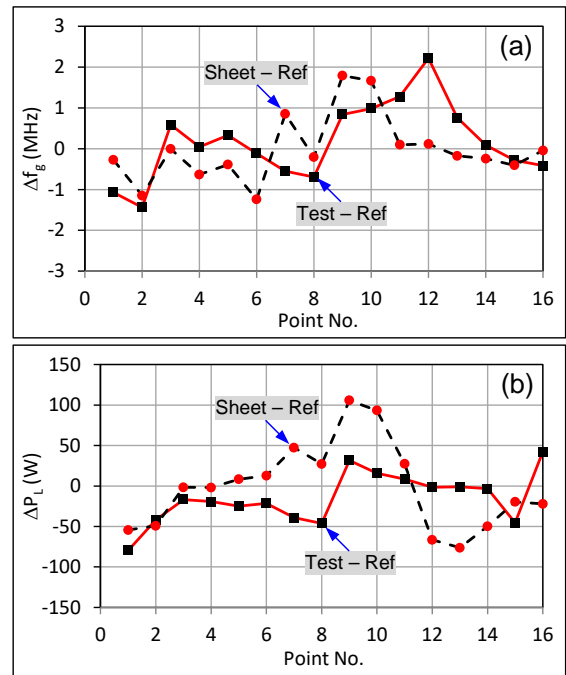
Figure 8. Deviations of generated frequency (Δf_g) and of delivered power (ΔP_L) from the reference setup measurements. Solid lines: test setup vs. reference setup. Dashed lines: datasheet vs. reference setup.

As a consistency check, dashed lines in Fig. 8 show differences between the values obtained from the magnetron datasheet and the reference setup measurements. While the frequency deviation is essentially the same, the RMS power deviation is slightly worse (50 W).

Given the combination of rather poor repeatability of installing the antenna probe to both of the launchers discussed before[2], which also applies to the magnetron, the deviations are sufficiently small to prove the validity of the proposed method. Further experiments are needed, with more sophisticated and automated data evaluation.

Conclusions

We have developed a method enabling real-time observation of a magnetron's Rieke-diagram related load reflection coefficient during full-power operation of any installation into which a high-power vector reflectometer (HPVR) can be integrated. To arrive at the Rieke reflection coefficient, the HPVR-measured reflection coefficient must be transformed by an appropriate equivalent linear two-port circuit. To obtain the circuit's scattering parameters, the following equipment must be available:

- Magnetron antenna probe associated with the given magnetron type
- Reference magnetron launcher (specified in magnetron datasheets)
- Launcher used in the installation (user launcher)
- Standard vector network analyzer (VNA)
- VNA calibration kit based on the reference launcher waveguide type
- VNA calibration kit based on the user launcher waveguide type

Two VNA calibrations must be performed, one with the probe installed in the reference launcher, the other with the probe installed in the user launcher. The two obtained scattering parameter sets can then be combined to arrive at the desired scattering parameters of the transforming equivalent two-port.

We have carried out verification experiments using a 2M244 magnetron, a customized WR340 waveguide launcher, and a WR340 waveguide-based HPVR. The comparison with direct measurement using the reference launcher as well as with the published Rieke diagram confirmed, within the experimental error, the validity of the devised method.

The proposed approach is useful for online monitoring of magnetron working conditions in installations where the magnetrons are not isolated from loads. This might prove beneficial when developing domestic or commercial microwave ovens or other circulator-less applications.

For Further Reading:

1. Meredith, R. J., Engineers' Handbook of Industrial Microwave Heating, London: The IEE, 1998, 250–270.
2. Bilik, V., On Proper Use of Magnetron Antenna Probes, *Proc. 3GCMEA*, Cartagena 2016, 116–121.
3. Engen, G., Microwave Circuit Theory and Foundations of Microwave Metrology, London: P. Peregrinus, 1992, 15–39.
4. Hackborn, R. A., An Automatic Network Analyzer System, *Microwave Journal*, 1968, **11**, No. 5, 45–52.

About the Author

Dr. Vladimir Bilik graduated in Radio-Electronics from the Slovak University of Technology at Bratislava in 1972, where he also received his PhD degree in 1979 and for more than two decades lectured courses on microwaves. Currently, he is responsible for R&D in S-TEAM company, which he co-founded in 1990, and still holds a part-time research fellowship with the University. His main professional interests have included automated scattering parameters measurement, implementations of six-port reflectometers, and automatic impedance matching of industrial microwave systems.